Hindawi
International Journal of Photoenergy
Volume 2022, Article ID 2024470, 16 pages
https://doi.org/10.1155/2022/2024470

Research Article

Long-Term Performance Analysis of Direct Photovoltaic Thermal-Assisted Heat Pump Water Heater Using Computational Model

Demiss Alemu Amibe[1] **and Alemayehu Tenaw Eneyaw**[2]

[1]*School of Mechanical and Industrial Engineering, Institute of Technology, Addis Ababa University, Addis Ababa, Ethiopia*
[2]*School of Mechanical and Chemical Engineering, Institute of Technology, Woldia University, Woldia, Amhara, Ethiopia*

Correspondence should be addressed to Demiss Alemu Amibe; demiss_a@yahoo.com

Received 15 October 2021; Revised 17 February 2022; Accepted 30 May 2022; Published 15 July 2022

Academic Editor: Carlo Renno

Copyright © 2022 Demiss Alemu Amibe and Alemayehu Tenaw Eneyaw. This is an open access article distributed under the Creative Commons Attribution License, which permits unrestricted use, distribution, and reproduction in any medium, provided the original work is properly cited.

The photovoltaic thermal system has a limitation in supplying hot water at the required temperature since it requires a supplementary heating system. One such system can be an air source heat pump operated by electricity from a PV/T system, which can be used to raise the temperature of the water preheated by PV/T to the required level. Such type system can also be called a hybrid PV/T-heat pump system, and it delivers thermal (hot water) and electrical energy. The performance of the hybrid PV/T-heat pump system was analyzed using the computational model for two Ethiopian cities, namely, Addis Ababa and Dire Dawa, which represent the highland and lowland regions, respectively. The simulation was conducted by inputting climatic data, daily hot water demand, and hourly hot water consumption patterns. Also, system design parameters such as PV/T area and peak Watt, PV/T warm water tank volume, air source heat pump water heater COP as a function of ambient temperature and circulating water temperature, and heat pump hot water tank volume. Besides, the effect of hot water consumption patterns (variability effect in three dissimilar cases constant, restaurant, and motel) on the system performance was examined. In addition, the effect of electric energy supply to the compressor of the heat pump using battery storage on the system performance was also investigated. In those diverse situations, the system in most of the cases generated hot water above 55°C and scored a COP of 3. The maximum value of hot water end-use efficiency of 66% was also obtained by making the hot water tank capacity about 50% of the daily hot water consumption size.

1. Introduction

Solar energy is utilized after it is converted into thermal energy and electrical energy. Traditionally, thermal energy is produced by solar thermal collectors and electrical energy is generated by photovoltaic (PV) systems. A hybrid photovoltaic/thermal (PV/T) system, which consists of a glazed photovoltaic panel with a flat plate absorber at the back, generates both electrical and thermal energies [1]. The purpose of the absorber is to cool the PV module so that the electrical efficiency can improve and convert the heat absorbed by the panel into useful thermal energy, as the absorber is not directly exposed to solar radiation and part of the radiation is converted into electrical energy. PV/T system has limitations in supplying hot water at the required temperature; usually, the maximum supply temperature is below 45°C. Overcoming this shortcoming requires a supplementary heating system. One such system can be an air source heat pump operated by electricity from a PV/T system, which can be used to raise the temperature of the water preheated by the PV/T to the required level [2].

Compared with fuel hot water boilers or electric water heaters, heat pump water heaters are more efficient and environment-friendly [3]. An air-source heat pump (ASHP) is a state of art heating system with many advantages, such as low energy consumption and relatively stable performance with huge energy-saving potential [4–6]. When PV electricity is used, it will have zero CO_2 emissions. A heat

pump water heater supplies water at the required temperature using an on/off or modulating control system of the compressor, and it can have also an electric heater backup integrated with the storage tank [7].

A combination of a heat pump and a photovoltaic thermal system generates hot water at the required temperature and electricity, and there are two types of possible wide-ranging configurations. In the first case, the photovoltaic thermal PV/T thermal collector is used as an evaporator and the condenser produces thermal energy, which is called direct photovoltaic thermal solar-assisted heat pump water heaters (PV/T-SAHP). Instead, if the PV/T is used to generate warm water that exchanges heat with the refrigerant in the evaporator of a heat pump, the system is called indirect PV/T-SAHP. In the second configuration, the PV/T collector is used to preheat water which will be further heated by the condenser of the air source heat pump water heater. Usually, literature groups PVT-HP system integration options into six major sections [8].

Over the past two decades, heat pump systems that use solar energy with different concepts were developed and investigated. One type of these systems is called indirect solar-assisted heat pump water heaters (SAHP). In such type of application, the solar flat plate collector serves as an evaporator to the heat pump that heats water using the heat released from the condensers and its COP was reported to reach 5 [9]. Extensive investigations were done on the performance of both direct and indirect PV/T-SAHP systems for water and space heating. The long-term performance of a solar-assisted heat pump for water heating applications was investigated [10], and the electrical energy consumption was reported to be 0.019 kWh/l. A PV/T-SAHP system where the PV/T collector is used as an evaporator of the heat pump was experimentally investigated and higher values of COP than air source heat pump at an average of 5-6 were obtained, while electric generation efficiency increased [11, 12].

The energy performance of a PV-SAHP system in Hong Kong has been examined based on a dynamic simulation model, it was found that the system could achieve a yearly-average COP of 5.93 and electricity efficiency of 12.1% (which is slightly better than the reference value at 25°C) [9]. Another researcher used an existing building to perform heating and cooling analysis for one year using the dynamic simulation model. As the simulation analysis results, the average coefficient of performance (COP) for the heating season was 5.3, and the average COP for the cooling season was 16.3, respectively [13]. Beyond the performance of the PVT-HP system enhanced, the system was also economically feasible and shortened the payback period compared to the standalone systems [14].

A PV/T-SAHP with a vapor injection cycle was proposed, fabricated, and investigated experimentally and better performance was obtained in winter conditions [15]. However, such a system is complex and will not function in months of very low solar irradiation. As PV/T collectors and air, source heat pump water heaters are available in the market and PV unit price is drastically falling; the two units can be configured in the right proportion to construct a hybrid PV/T-heat pump system to meet a specified hot water and electricity load. Generally, the PVT-HP system performed satisfactory performance to deliver hot water at the required temperature year-round [16]. The system is not limited to generating hot water, electricity, and building air conditioning whereas it is functional for milk pasteurization in good performance [17].

Air source heat pump water heaters using grid electricity are widely used for domestic water heating, swimming pool heating, and commercial water heating. Following the international trend, several air source heat pump water heaters were installed in 2–4-star hotels in Ethiopia in the last decade. One of the recent review articles in the title concluded the benefit of the system integration in one sentence by saying overall energy performances are comparable and even better than those of conventional air-source and water-source systems. The integration of PVT collectors and HPs improves the performance of both subsystems, increasing solar energy exploitation and HP efficiency while reducing defrosting cycles in air-source HPs [18]. PVT-HP systems rarely use the exhaust air as the source of heat for the integrated system [19].

The main novelty of this work is that the PV/T system is used as a source of electrical energy for the compressor of the heat pump water heater and used a PV/T collector as a water preheater for the air source heat pump water heater rather than an evaporator (refrigerant fluid circulated in the PV/T collector) of the heat pump. The preheated water by the PV/T collector is circulated through the heat pump condenser for further water temperature increment to the required level.

2. System Description

The integrated hybrid photovoltaic thermal and heat pump water heating system for this research consists of a PV/T system that generates warm water and electricity and an air-to-water heat pump that heats the warm water from PV/T and generates hot water as shown in Figure 1. The warm water from the PV/T storage tank is transferred to the heat pump hot water tank as hot water is consumed and recirculated by a pump through the condenser of the air source heat pump until the temperature reaches the hot water supply temperature. The compressor of the heat pump runs by electricity supplied from the PV/T. The system can be configured in such a way only to supply hot water or both electricity and hot water. In the first case, the PV/T will generate sufficient electricity in the critical month to run the compressor of the heat pump so that it can boost and deliver the required hot water using the system configuration. In the second case, it will generate electricity not only to run the air source heat pump water heater but also, it will supply additional electricity for different applications such as lighting and refrigeration. Hence, the system can be used for off-grid areas.

3. Mathematical and Computational Model

One possible path of prediction of the performance of the PV/T-heat pump system shall consist of the following steps:

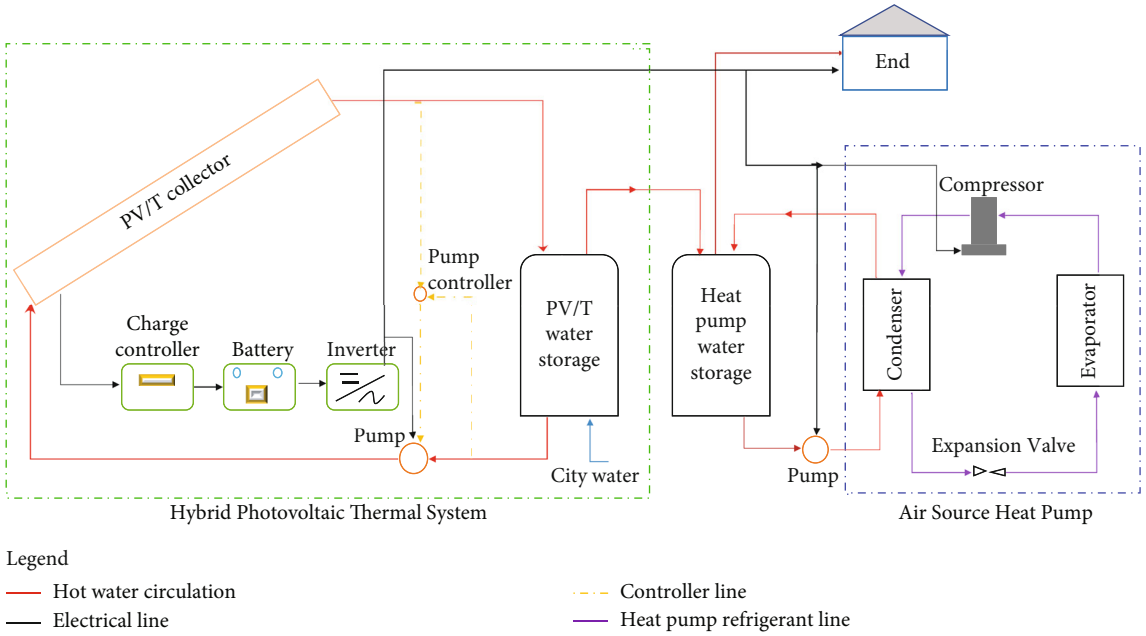

Figure 1: Schematic diagram of hybrid photovoltaic thermal heat pump system.

(i) Determination of instantaneous electrical power generation by PV panel depending on solar radiation and panel temperature

(ii) Computation of temperature of water in the absorber outlet and PV/T water tank

(iii) Determination of the heat transferred to the water in heat pump tank from the refrigerant and eventually considering hot water supply to end-user and dilution by make-up water from the PV/T tank

In this work, the PV/T model is coupled with an air source heat pump water heater model. Input parameters for dynamic simulation of the heat pump operation are hourly values of the ambient temperature for a year, daily hot water consumption volume, hourly hot water consumption pattern, hot water storage tank volume, heat loss coefficient of storage and surface area, instantaneous electrical power generation by PV/T and PV/T water tank temperature from the PV/T model, and COP general relation from the manufacturer of the heat pump.

3.1. Mathematical Model

3.1.1. PV/T System Mathematical Model. The PV/T mathematical model is adopted from the previously published paper by the authors [20].

The isotropic diffuse model radiation on a tilted surface considering beam, isotropic diffuse, and solar irradiance reflected from the ground is given as follows [21]:

$$I = I_b R_b + I_d\left(\frac{1+\cos\beta}{2}\right) + I\rho_g\left(\frac{1-\cos\beta}{2}\right). \quad (1)$$

(1) Glass Cover. The energy balance of solar irradiance absorbed by the glass plus the heat received from the PV module by the glass and the heat leaving the glass to the ambient gives the rate of change of energy stored in the glass cover as follows [22, 23]:

$$(m_c)_g \frac{\partial T_g}{\partial t} = A_{pv}\left[I_c(\alpha)_g + U_{pv-g}\left(T_{pv} - T_g\right) - U_{g-a}\left(T_g - T_a\right)\right]. \quad (2)$$

(2) PV Module. The rate of change of energy stored in the PV module is obtained as the difference between solar irradiance absorbed by the PV module, the heat transferred from the PV module to glass and absorber, and also electrical energy generated by the PV module [24].

$$\begin{aligned}(m_c)_{pv}\frac{\partial T_{pv}}{\partial t} = {} & A_{pv} I_c \tau_g \alpha_{pv} - P_{el} - A_{pv}\frac{k_{pv}}{\delta_{pv}}\left(T_{pv} - \eta_f T_p\right) \\ & - A_{pv} U_{pv-g}\left(T_{pv} - T_g\right) \\ & - A_{pv} U_{pv-a} x\left(T_{pv} - Ta\right).\end{aligned} \quad (3)$$

(3) Absorber Plate. The difference between the heat transferred to the absorber from the PV module and the sum of heat transferred from the absorber to the water in the tubes and the ambient through the back of insulation results in the rate of change of energy stored in the absorber [25].

$$(m_c)_p \eta_f \frac{\partial T_p}{\partial t} = \left(A_{pv} \frac{k_{pv}}{\delta_{pv}} \left(T_{pv} - \eta_f T_p\right)\right) - A_{wt} U_{p-w} \left(f_w \times T_p - \frac{T_{w,o} + T_{w,i}}{2}\right) - A_{pv} U_{i-a} \left(\eta_f T_p - T_a\right). \quad (4)$$

It shall be noted that η_f is fin efficiency of the absorber plate to the tube, T_p is the maximum absorber temperature, $\eta_f T_p$ is the mean absorber temperature, and $f_w = (2\eta_f - 1)$ is a factor that is used to determine water tube temperature from maximum absorber temperature.

(4) Water Outlet Temperature from Absorber Plate. The rate of change of internal energy of the water inside the tube is obtained from the difference between the heat transferred from the absorber to the water in the tubes and heat transported with water from the tube to the storage [24].

$$m_w c_w \frac{\partial T_w}{\partial t} = A_{wt} U_{p-w} \left(f_w \times T_p - \frac{T_{w,o} + T_{w,i}}{2}\right) - \dot{m}_w c_w (T_{w,o} - T_{w,i}) \quad (5)$$

(5) Storage Tank. Similar to Equation (5), the rate of change of energy stored in hot water in the tank is obtained as follows:

$$m_w c_w \frac{\partial T_{st}}{\partial t} = m_w n c_w (T_{w,o} - T_{w,i}) - \text{dhwc} \times c_w \times F F_{ii} (T_{st} - T_{ws}) - U_{st-a} A_{st} (T_{st} - T_a). \quad (6)$$

3.1.2. PV/T System Computational Model. The above transient ordinary differential equations are solved by the explicit finite difference time-stepping scheme below.

(1) Glass Cover. Expressing the overall heat transfer coefficient in terms of convective and radiative components, the glass temperature at the current time step is obtained as follows by discretization of Equation (2):

$$T_{g,i+1} = T_{g,i} + \frac{\Delta t}{m \times c_p} A_c \left(I_c \alpha_g - \left(h_{c,g-a} + h_{r,g-a}\right) \times \left(T_{g,i} - T_{a,i}\right) + \left(h_{c,pv-g} + h_{r,pv-g}\right) \times \left(T_{pv,i} - T_{g,i}\right)\right). \quad (7)$$

The radiation and convection heat transfer coefficients at the top and bottom parts of the glass are given as follows [26]:

$$h_{r,g-a} = \sigma \varepsilon_g \left(T_{sky}^2 + T_g^2\right)\left(T_{sky} + T_g\right), h_{r,pv-g} = \frac{\sigma \left(T_g^2 + T_{pv}^2\right)\left(T_g + T_{pv}\right)}{\left(1/\varepsilon_{pv}\right) + \left(1/\varepsilon_g\right) - 1}, \quad (8)$$

$$h_{c,g-a} = 2.8 + 3V_{wind}, \quad (9)$$

where $T_{sky} = T_a - 6$ taken as per the reference [26] quantified in what way the two temperatures functioned.

The convection heat transfer coefficient Equation (8) depends on wind velocity [27].

(2) PV Module. The PV module average temperature at the new time step is obtained as follows by discretization of Equation (3).

$$T_{PV,i+1} = T_{PV,i} + \frac{\Delta t}{(m_c)_{PV}} A_c \left[I_c - P_{el,i} - \frac{k_{PV}}{t_{PV}} A_{PV-P} (T_{PV,i} - \eta_f T_{P,i}) - \left(h_{c,PV-g} + h_{r,PV-g}\right)\left(T_{PV,i} - T_{g,i}\right)\right]. \quad (10)$$

(3) Absorber Plate. By discretizing Equation (4), the maximum temperature of the absorber plate at the new time step is expressed as follows:

$$T_{P,i+i} = T_{P,i} + \frac{\Delta t}{\eta_f (m_c)_P} \left[\frac{k_{PV}}{t_{PV}} A_{PV,i} (T_{PV,i} - \eta_f T_{P,i}) - \frac{\Delta t}{\eta_f (m_c)_P} (A_{wt} U_{P-w}) \left(F_w (2\eta_f - 1) T_{P,i} - \frac{T_{wo,i} + T_{wi,i}}{2}\right) - U_{P-i} A_P (\eta_f T_{P,i} - T_{a,i})\right]. \quad (11)$$

(4) Water Outlet Temperature from Absorber Plate. The outlet temperature of the water from the absorber at the new time step is given as follows by discretizing Equation (5):

$$T_{wo,i+1} = T_{wo,i} + \frac{\Delta t}{(m_c)_w} \left[A_{wt} U_{p-w} \left((2\eta_f - 1) T_p - \frac{T_{wo,i} + T\text{wi}, i}{2}\right) - \dot{m}_w c_w (T_{wo,i} - T_{wi,i})\right]. \quad (12)$$

(5) Storage Tank. Discretization of Equation (6) yields the water temperature in the storage at the new time step as follows:

$$T_{stw,i+i} = T_{stw,i} + \frac{\Delta t}{C_w \rho_w V_{st}} [m_w n c_w (T_{wo,i} - T_{wi,i}) - [U_{st-a} A_{st} (T_{stw,i} - T_{a,i}) + \rho_w V_{st} \text{dhwc} \times F F_{ii} (T_{stw,i} - T_{ws})]]. \quad (13)$$

3.1.3. The Useful Thermal Energy of the Heat Pump. Equation (14) states the heat transported by the heat pump system from ambient to the hot water storage tank without electrical battery storage when the power generated by PV/T is directly consumed by the heat pump [28]. Similarly, Equation (15) evaluates the heat transported by the heat pump to hot water using battery storage. In this case, an hourly schedule for electric energy consumption is necessary and included in the equation for the simulation.

$$\dot{Q}_{HP} = \text{COP}_{HP} \times P_{el}, \quad (14)$$

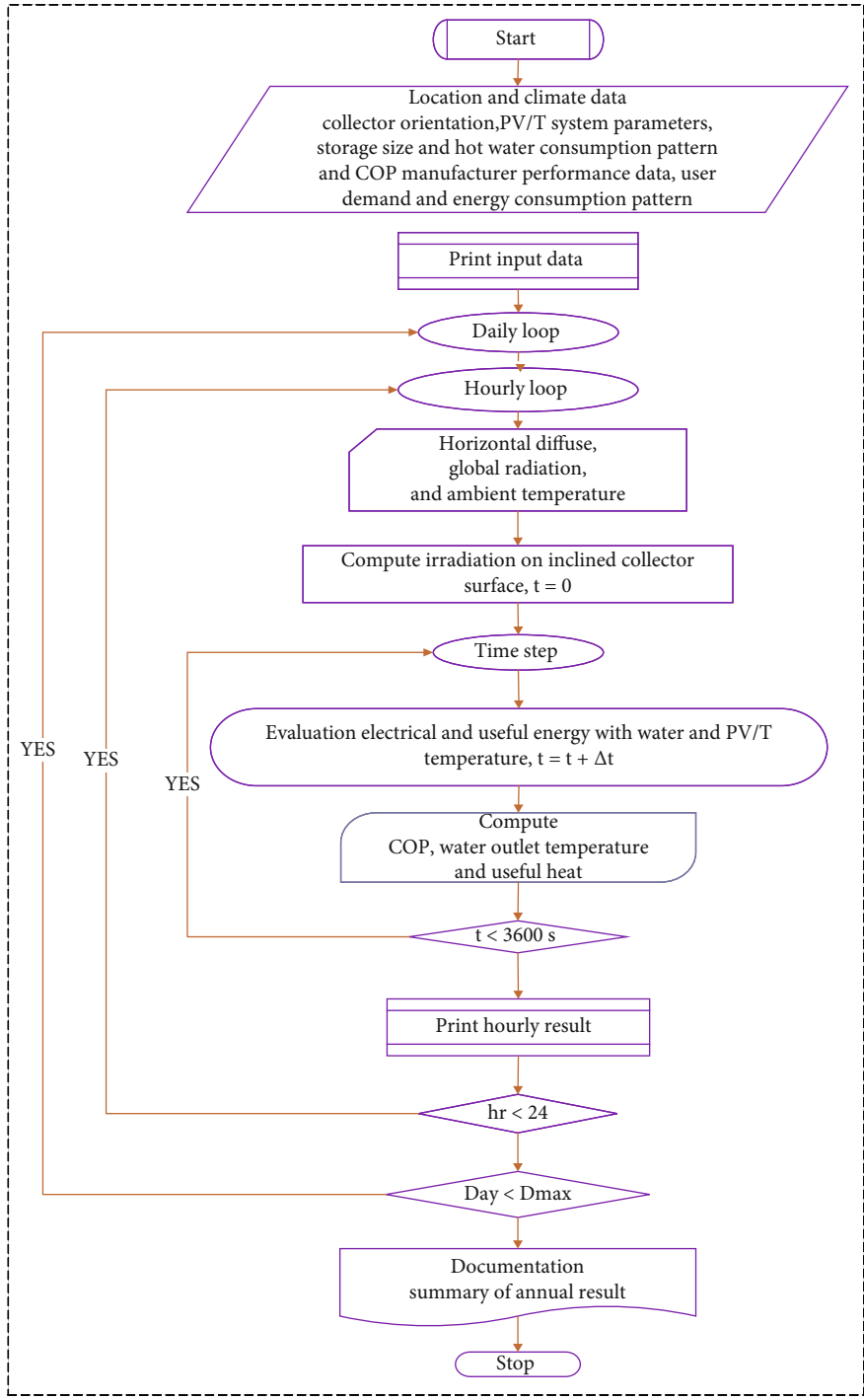

Figure 2: Hybrid PV/T heat pump system algorithm.

$$\dot{Q}_{HP} = COP_{HP} \times P_{el} \times f_{HP}. \quad (15)$$

3.1.4. Hot Water Storage Tank Temperature. The temperature of hot water in the heat pump storage tank is determined by the net heat gain of the hot water tank. The net heat gain of the storage tank is equal to thermal energy transported by the heat pump from ambient to the hot water tank subtracting the difference of enthalpy of thermal energy of hot water supplied to the end-user and warm make-up water from the PV/T water tank and the heat lost to the ambient across the wall of the storage tank.

$$T_w^{n+1} = T_w^n + \frac{Q_{hp} - (DWC \times C_w \times ff(j)) \times (T_{,w}^n - T_{s1}) - U_{ls} \times A_{st} \times (T_w^n - T_a))}{\rho_w \times V_{dot} \times C_w}. \quad (16)$$

3.2. Computer Program Flow Chart. The flow chart of the computer program is given in Figure 2 comprising the two

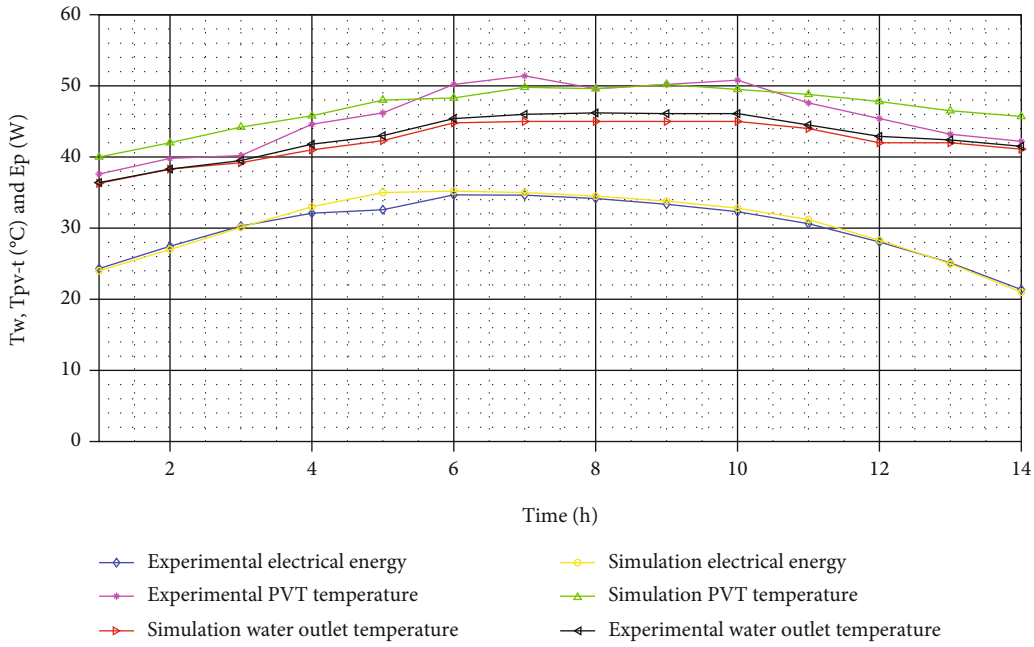

Figure 3: Verification result of the PV/T experimental and the simulation results.

subsystems: the hybrid photovoltaic thermal and air source heat pump water heater. As we can see in the flow chart, the primary target of the PV/T system module is to determine electrical and thermal (hot water) energy generation by PV/T which is used as an input to the heat pump water heater.

The computational analysis starts by converting the solar irradiation at a horizontal surface to solar radiation on the inclined PV/T surface at every time step. Then, using the generated PV/T electrical energy and warm water temperature, the ambient temperature of the site, manufacturer performance data of heat pump, daily hot water consumption volume, and hourly hot water consumption pattern, the hot water supply temperature is determined. The computer program can be used to see whether a given system configuration meets design requirements or not. As shown in the flow chart, the developed MATLAB program delivers the heat pump generated thermal energy, hot water temperature, and COP at every time step. Year-round or 8760 hours of simulation has to be conducted to determine the annual performance of the system.

3.3. Verification of the PV/T and COP Formula of the Heat Pump. The photovoltaic thermal part was verified through an experimental paper result as a standard for the hybrid photovoltaic thermal system [29]. The verified result of the PV/T was previously published by the authors [20] and a part of the author dissertation [30]. Also, the researcher verified the heat pump system using the coefficient of performance curve generated from the heat pump manufacturer data.

Figure 3 compares the experimental and simulation results for electrical energy generation, water outlet temperature, and PV/T surface temperature. In all cases, simulation and experimental results are in good agreement with an average error of 1.77%, 2.3%, and 3% for electrical energy, water outlet, and PV/T surface temperature, respectively.

Table 1: COP of the heat pump as a function of ambient and hot water temperature.

Ambient temperature (°C)	Inlet water temperature (°C)				
	25	32	40	43	50
7	4.05	3.5	2.92	2.7	1.98
15	4.76	4.22	3.62	3.32	2.68
25	5.82	3.36	4.41	3.36	3.1
35	—	—	4.72	4.31	3.4

The main difference between the previously published article by the authors and this paper was the integration of the heat pump into the hybrid photovoltaic thermal system. The hybrid photovoltaic thermal system alone cannot deliver the required thermal and electric needs of the end-user at the required hot water temperature. Integrated heat pump to the hybrid photovoltaic thermal system supports the generation of the required hot water and improves the performance of both the photovoltaic thermal collector and the heat pump system. The current article verified the additional heat pump part using manufacturer data.

The system was evaluated as a year-round capability to deliver both electricity and hot water. The system coefficient of performance is based on the system generation capacity. The COP of the heat pump relates to the output or the heat transported by the condenser per unit time for water heating divided by the input which is the electrical power input into the compressor stated in Equation (17). As stated below, the COP of a heat pump water heater is given as a function of ambient air temperature and hot water temperature inlet

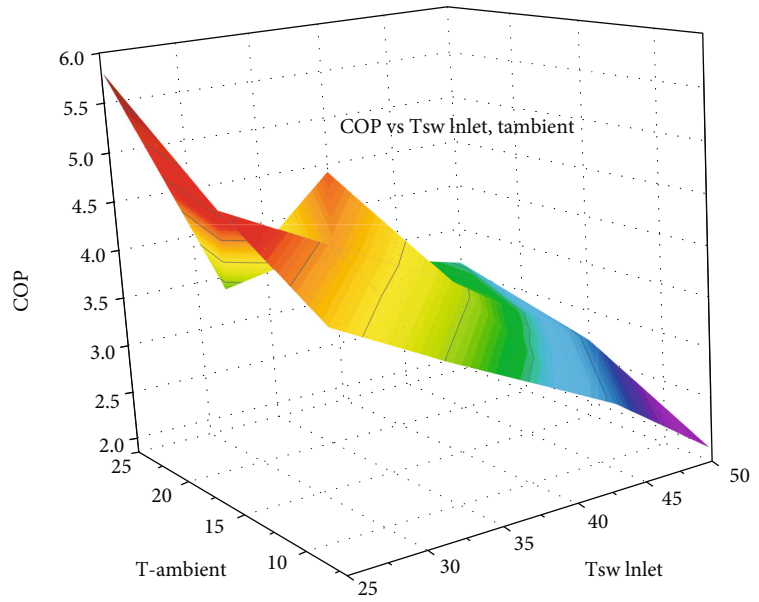

Figure 4: COP as a function of ambient and heat pump hot water tank temperature.

temperature to the condenser by the manufacturer which is given in Table 1.

$$\mathrm{COP_{HP}} = \frac{\dot{Q}_{\mathrm{HP,out}}}{P_{\mathrm{el,in}}}. \tag{17}$$

Using the parameters in Table 1, a 3D surface was developed using a curve fitting application, and the following equation of COP was obtained as a function of hot water temperature and ambient temperature and illustrated in Figure 4. From the surface generated, the COP equation is presented in the following equation:

$$\mathrm{COP} = \begin{pmatrix} 0.4641 - (0.36538 \times T_{s2i}) - 0.13596 \times T_a - 0.01164 \times T_{s2i}^2 + 0.004564 \times T_a \times T_{s2i} \\ +0.008122 \times T_a^2 + 0.00009655 \times T_{s2i}^3 + 0.0003286 \times T_{s2i}^2 \times T_a - 0.2829 \times T_{s2i} \times T_a^2 \end{pmatrix}. \tag{18}$$

4. Results and Discussion

4.1. Hybrid PV/T Heat Pump at the Different Climatic Conditions. For the comparison of different climatic conditions in tropical areas, Dire Dawa is selected to represent the hot climate of the lowland and Addis Ababa's mild climate of the highland. The comparison is performed for the hot season taking the solar irradiation and ambient temperature of May for Dire Dawa and Addis Ababa. Parameters that have a major influence on the system performance such as PV/T area, PV/T tank capacity, heat pump capacity, and hot water tank capacity as well as daily hot water consumption volume and hot water consumption patterns were made the same for both sites. As for performance indicators, the coefficient of performance and hot water temperature in the storage tank as well as the hot water end-use efficiency are used and the technical data of the system equipment is specified in Table 2.

Figure 5 shows the results of the simulation of the hybrid PV/T heat pump water heating system for Dire Dawa and Addis Ababa for May. The hot water supply temperature of Dire Dawa is higher than that of Addis Ababa in all 24 hours of the day. At 9:00 h, the hot water temperature reached 70°C and 52°C, respectively, for Dire Dawa and Addis Ababa then both started to decrease. This happened because the ambient temperature and other affecting parameters were better in Dire Dawa relative to Addis Ababa.

Again, the COP of the heat pump at Dire Dawa was better than that of Addis Ababa due to the higher ambient temperature. It shall be noted that the heat pump is not operating during the night as electric power is not generated by the PV/T unless the system is integrated with battery storage.

The results show that Dire Dawa is a better and more appropriate site for the application of a hybrid PV/T heat pump water heating system application than Addis Ababa. When the water temperature reached the highest temperature, the COP dropped to about 2 in Dire Dawa and 1.7 in Addis Ababa. The average COP during the day was above 3.5 in Dire Dawa and about 3 in Addis Ababa.

The evaluation of annual end-use efficiency for a different storage volume is given in Table 3. The results show that

Table 2: Technical data of the hybrid PV/T heat pump system used for simulation.

	Description	Unit	Value
Heat pump	Model		FAR-01S
	Heating capacity	Kw	3.6
	Hot water supply	L/H	75
	Unit weight	kg	35
	Refrigerant type		R410A
Water storage	Capacity	Liter	500
	Color		Stainless steel
	Maximum pressure	kPa	1000
PV/T	Each module area	m^2	1.654
	Total area	m^2	20

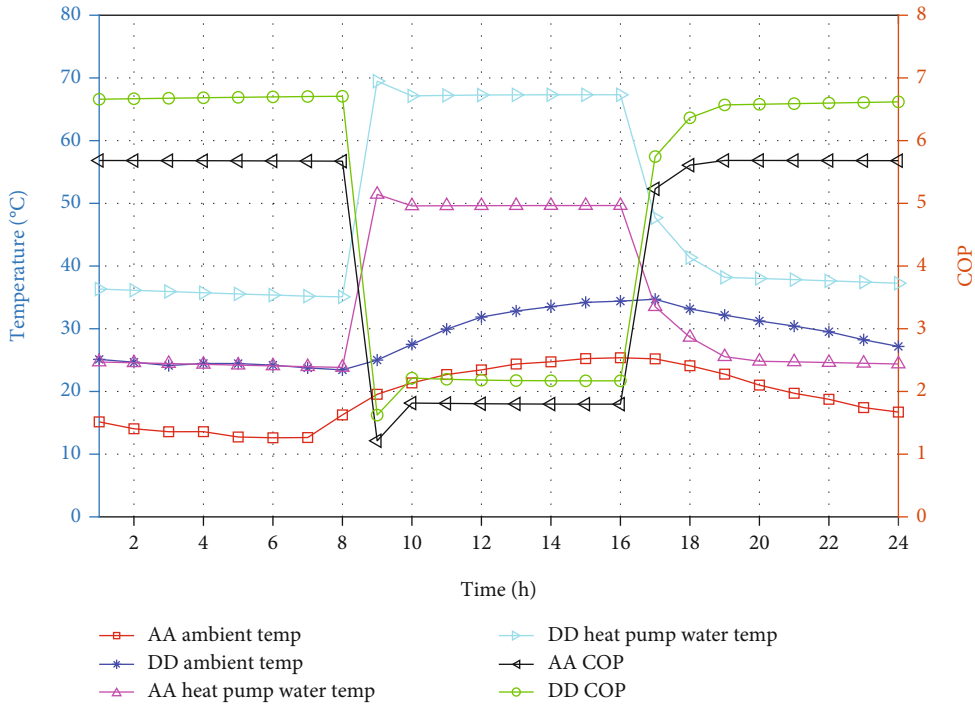

Figure 5: Comparison of performance of hybrid PV/T heat pump system in Dire Dawa and Addis Abba under constant hot water supply conditions during office hours.

Table 3: Annual hot water end-use efficacy of Dire Dawa and Addis Ababa.

	Thermal efficiency of PV/T	End-use efficiency			
		Storage volume 4.8 m^3		Storage volume 2.4 m^3	
		PV/T	PV/T heat pump	PV/T	PV/T heat pump
Dire Dawa	51.34%	37.54%	63.69%	38.59%	66.77%
Addis Ababa	47.03%	29.01%	61.24%	29.81%	64.32%

an improvement of 3% is obtained by making the hot water supply tank half of the daily hot water consumption.

4.2. Effect of Hot Water Consumption Pattern on System Performance. The effect of hourly hot water consumption patterns of the end-user for a restaurant, motel, and health center on the system performance was analyzed for Dire Dawa. The hourly hot water fraction pattern for the different cases is illustrated in Figure 6. Their effect on COP of heat pump, hot water supply temperature, and hot water end-use efficiency is discussed in the following paragraphs.

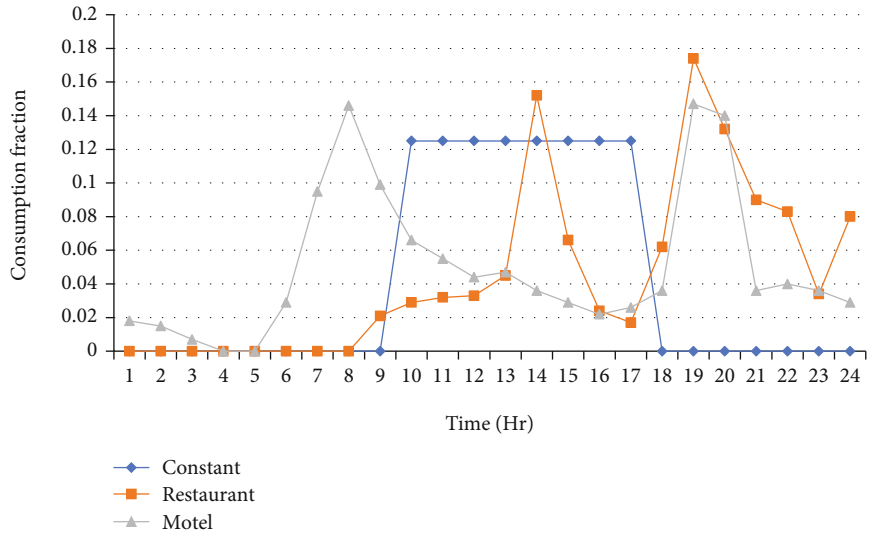

Figure 6: Hot water consumption pattern for three selected cases.

Table 4: COP of the heat pump on selected days by taking max and minimum.

Fraction type	Constant		Restaurant		Motel	
Selected month	Maximum June 11	Minimum January 17	Maximum June 11	Minimum January 17	Maximum June 11	Minimum January 17
Minimum	1.62	1.11	1.72	1.15	1.97	1.33
Maximum	6.85	6.06	6.78	6.06	6.78	6.07
Average	5.2	4.4	5.17	4.26	5.21	4.3

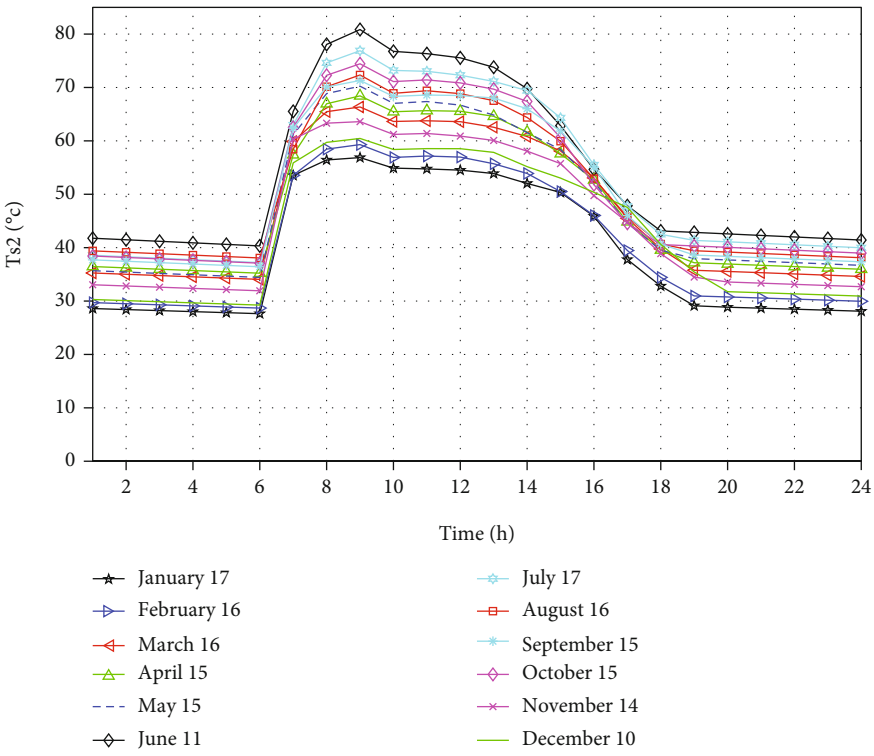

Figure 7: Storage water temperature in the case of constant consumption pattern.

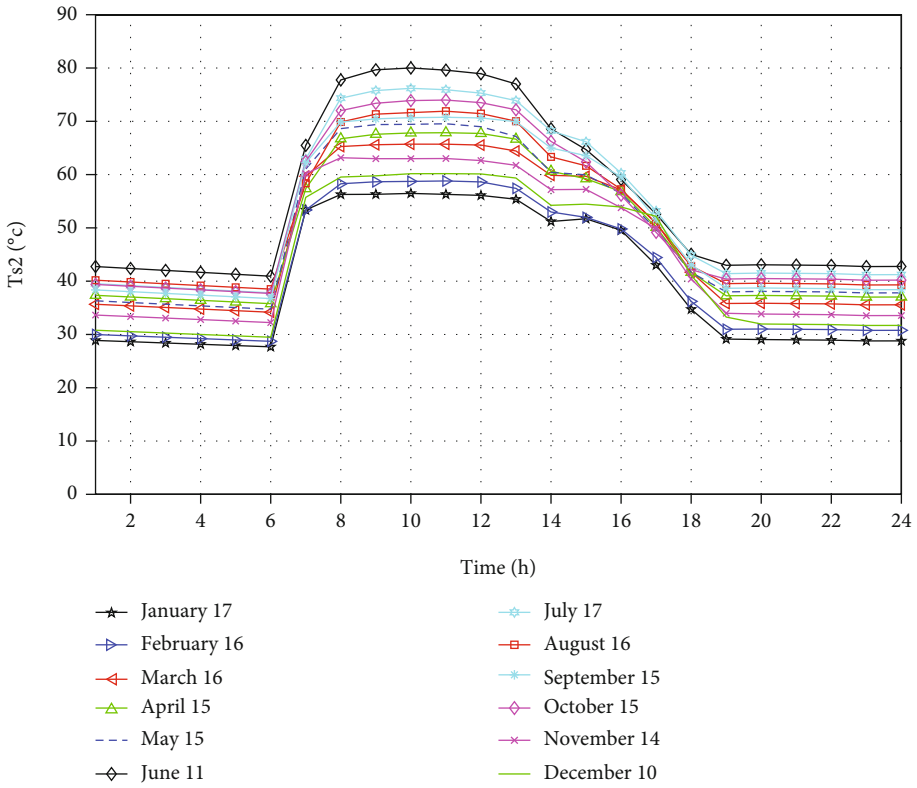

Figure 8: Storage water temperature at restaurant consumption pattern.

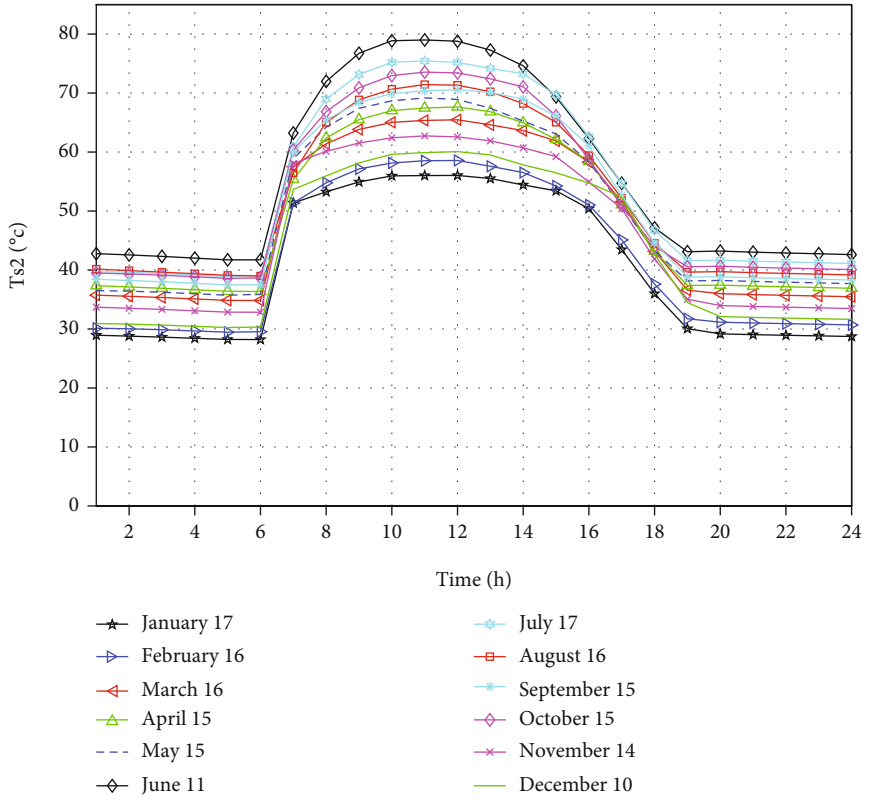

Figure 9: Storage water temperature for motel consumption pattern case.

Table 5: Temperature summary of the heat pump by taking max and minimum.

Fraction type	Constant		Restaurant		Motel	
Selected month	Maximum June 11	Minimum January 17	Maximum June 11	Minimum January 17	Maximum June 11	Minimum January 17
Minimum (°C)	41.4	28.39	42.16	28.5	42.29	29.6
Maximum (°C)	80.83	57.16	80.52	57.04	79.33	56.5
Average (°C)	54.65	39.55	55.87	40.32	55.71	40.2

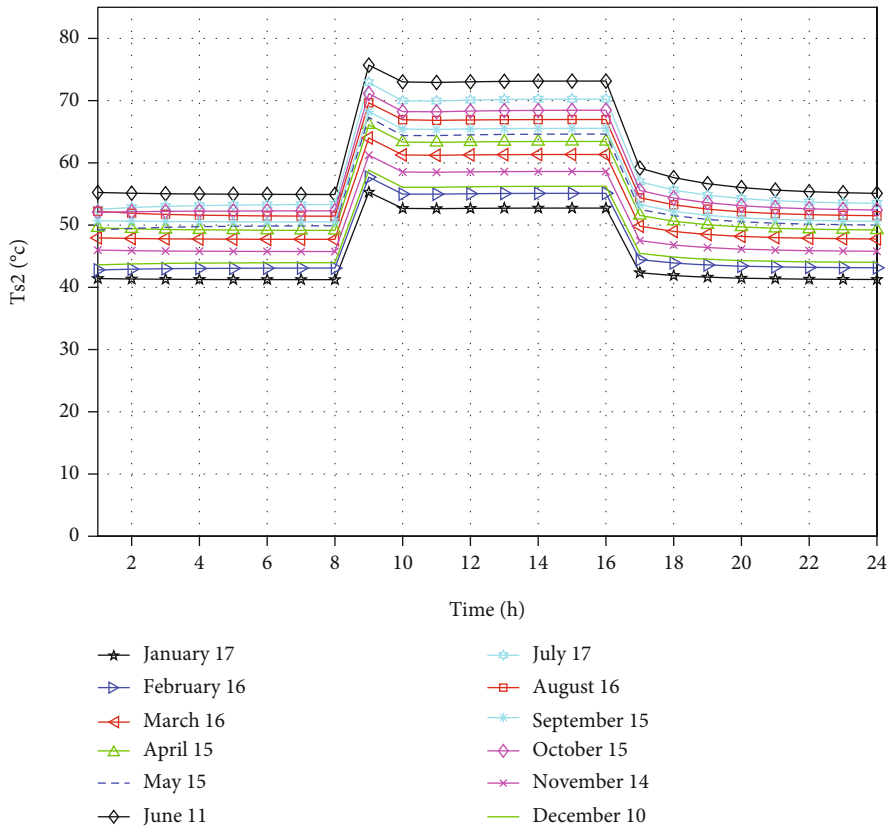

Figure 10: Water temperature with 75% electrical energy supply during 8 hours of water supply hours and 25% during the rest.

Table 4 shows the variation of COP for different hot water consumption pattern cases on directly supplied PV/T system-generated electrical energy to the heat pump.

Similar to the COP of the heat pump, the hot water supply temperature was compared for three types of consumption pattern cases (constant, restaurant, and motel).

4.2.1. Constant Consumption Pattern Case. In this case, the maximum hot water temperature generated by the heat pump and stored in the tank rose age up to 80°C as shown in Figure 7. As the solar irradiation decreased between 13:00 and 17:00 hours of the day, the end-user hot water temperature dropped between 40 and 55°C; during the evening, the temperature further dropped.

4.2.2. Restaurant Case. In a restaurant consummation pattern, hot water at 55–80°C is supplied from 8 to 13 hours to the end-user during the year as shown in Figure 8 and then, the hot water temperature dropped drastically from 13:00 to 17:00 hours reaching 42-50°C.

4.2.3. Motel Case. In the motel consumption pattern case, the hot water temperature was delivered at 55–80°C to the end-user from 8 to 13 hours during the year as shown in Figure 9. At night time, the required hot water temperature was not achieved due to the absence of electric power to the heat pump. To eliminate this problem, the hot water tank with controlled mixing with make-up water with two levels can be considered to avoid thermal degradation. Another alternative is using the battery for electrical energy.

Table 5 shows a comparison of the hot water supply temperature of the three hot water hourly consummation patterns. Although the difference is insignificant, the restaurant case seems to have the best performance.

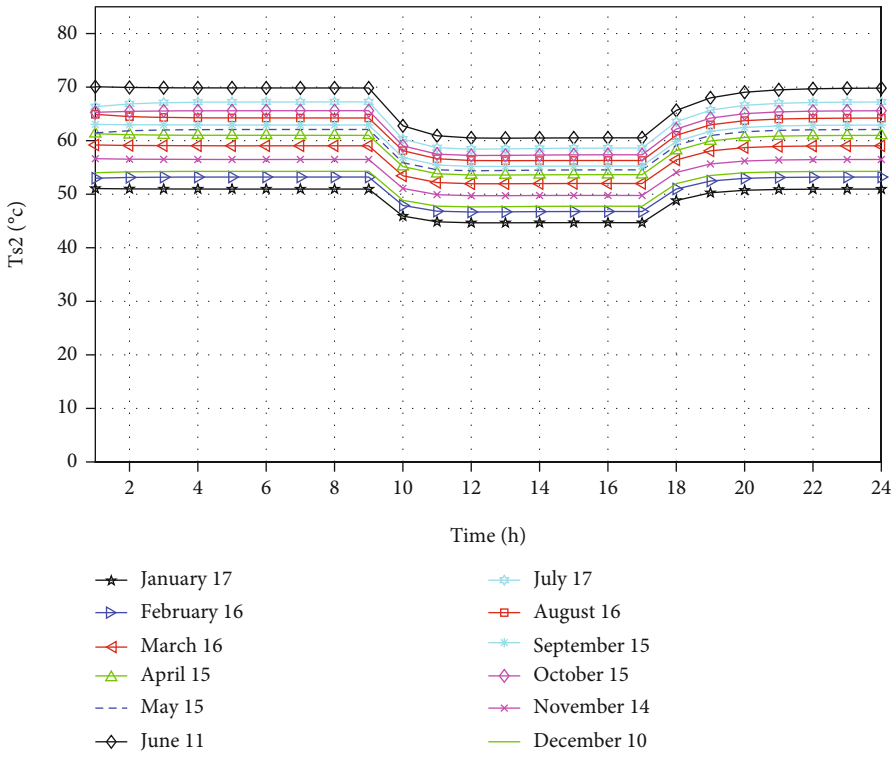

Figure 11: Water temperature for constant power supply energy option in 24 hours using battery storage and 8 hours of hot water consumption at a constant rate.

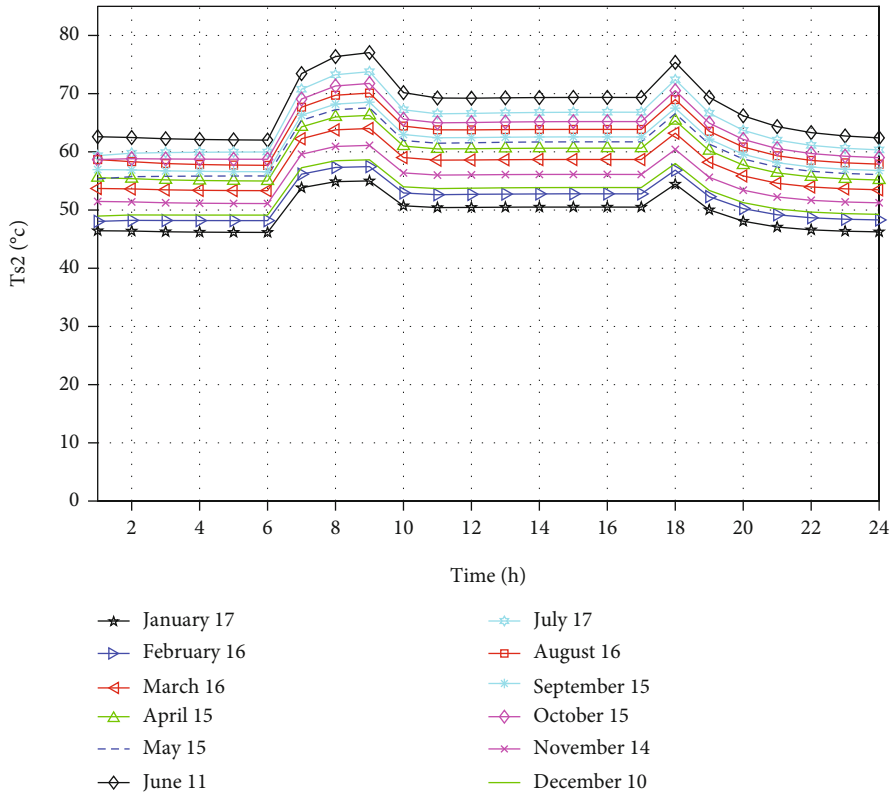

Figure 12: Water temperature with 75% electrical energy supply during 12 hours of the day and 25% during the rest.

Table 6: Temperature of selected days in different energy supply cases.

General classification	Energy supply	Selected days	Minimum (°C)	Maximum (°C)
Baseline	No battery	11-Jun	41	80
		17-Jan	28	57
75% in 8 hot water supply hours	25/75	11-Jun	53.5	77.2
		17-Jan	40.16	55.66
24-hour uniform		11-Jun	63.23	70.32
		17-Jan	46.67	51.2
75% in 12-hour daytime		11-Jun	58.68	75.26
		17-Jan	43.93	54.00

Table 7: COP summary for different cases on a selected day.

General classification	Energy supply	Selected days	Minimum	Maximum
Baseline	0%	11-Jun	2.00	6.94
		17-Jan	1.29	6.07
8 h/16 h	75/25%	11-Jun	2.4	5.94
		17-Jan	1.6	5.13
24 h uniform	100%	11-Jun	3.67	4.77
		17-Jan	2.88	3.96
12/12 h	75/25%	11-Jun	2.78	5.36
		17-Jan	2.1	4..51

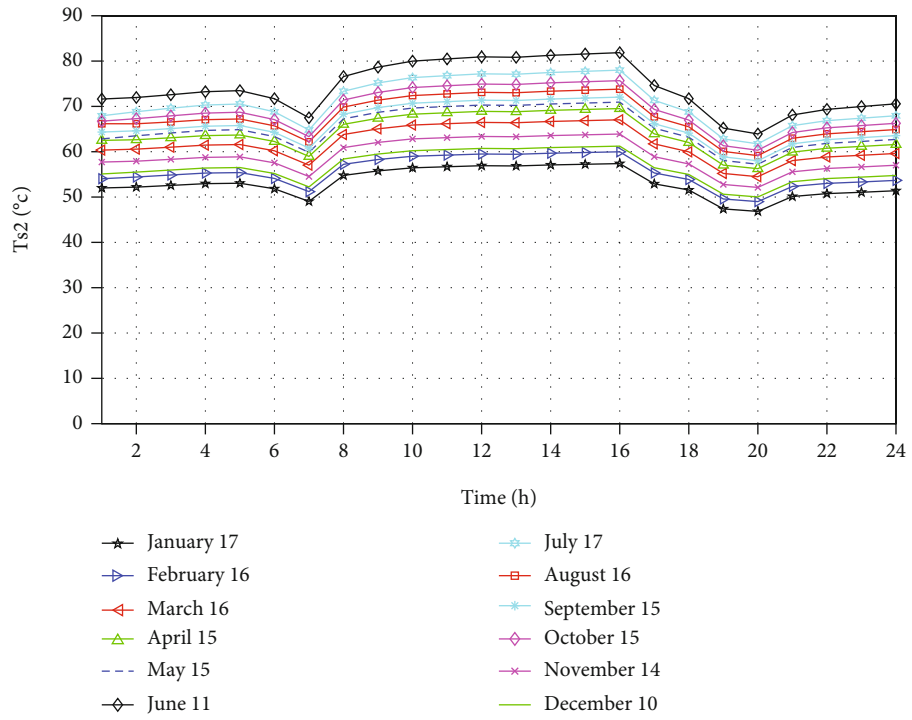

Figure 13: Water temperature in motel consumption with 1/3 of electrical energy storage in the battery for nighttime.

4.3. Effect of the Electrical Energy Storage Battery on Hot Water Supply Temperature. In this section, the option of storing electrical energy to level the variation of hot water temperature and delivering at the required time and temperature to the end-user is investigated. The hourly hot water consumption pattern that is used for the simulation is the constant consumption case for 8 hours.

In the first case, 75% of the electrical energy is utilized during 8 hours of hot water supply and 25% of the electrical energy is used for 16 hours of the day. Compared to the

results of Dire Dawa in Figure 7, the results of this investigation in Figure 10 show that the hot temperature increased in the early morning and evening. Even in the coolest month, the hot water temperature was above 45°C.

Figure 11 shows the obtained water temperature variation when the power supply to the compressor is made constant through 24 hours of the day and hot water is consumed during the day from 9 to 17 h at a constant rate. The conclusion is that the water temperature in the tank is leveled and such type of power supply is more suitable for the water heating system with considerable evening and early morning loads.

Figure 12 shows hot water temperature variation when the 75% power supply to the compressor is made constant through 12 hours (6 h-18 h) of the day using battery electrical storage for PV and hot water consumption from 9 h to 17 h at a constant rate. From the figure, it can be concluded that the water temperature in the tank is almost constant from 7 h to 20 h which is more appropriate for application with a considerable hot load during the day. The temperature summary of the three cases with the baseline data or no-electrical energy storage is given in Table 6.

For different cases of storage and supply of electricity, COP maximum and the minimum values for representative days of the hot and cool season are given. In Table 7, the result shows that the gap between maximum and minimum COP values decreased when the electrical energy supply is made more uniform.

In Section 4.2, it was shown that for the motel case hot water consumption, the required hot water temperature was not met especially in the cooled season due to considerable high hot water consumption during the night, because of the electrical energy supplied to the HP compressor without being stored in the battery only during the PV/T working time. To solve this problem, integrating electrical battery storage into the system is considered a solution.

After several trials, a PV/T heat pump system with an increase of 20% in size from the baseline and integration of a battery system for storing about one-third of electrical energy generated hours for supply in the PV/T off-time or night time and delivered hot water temperature above 50°C in the cold season as illustrated in Figure 13.

5. Conclusion

The computational model of the PV/T heat pump integrated hybrid system developed during the research was used to analyze the performance of hybrid PV/T heat pump systems for different applications and different tropical climate conditions. The computations were done using the MATLAB program considering heat pump energy consumption options, different tropical climatic conditions, and variability of the end-user (constant, restaurant, and motel) hourly hot water fraction pattern. The simulation results of the system consisted of COP, hourly hot water temperature, and hot water end-use efficiency for selected days of each month.

Beyond the impact of hot water consumption patterns, using electrical storage and supply hot water tank size, the effect of the different climatic conditions within tropical areas such as lowland and moderate highland was seen. The nominated sites Addis Ababa and Dire Dawa are representative of the moderate highland and lowland site of Ethiopia, respectively. According to the results, a hybrid PV/T heat pump hot water production system is highly recommended for hot sites like Dire Dawa relative to Addis Ababa.

As per the results, the hybrid PV/T heat pump water heater can deliver a maximum of 80°C hot water and an average hot water temperature of 55°C and above. The generated water temperature by the PVT-HP system performed by this research paper aligned with the experimental hybrid photovoltaic thermal and heat pump system for public hospitals [31]. The generated water temperature was above the conventional 45°C hot water temperature [32]. The maximum value of hot water end-use efficiency of 66% was also obtained by making the hot water tank capacity about 50% of daily hot water consumption.

Whenever the hot water demand during the day working hours is constant, the hybrid PV/T heat pump system can supply hot water without a backup system in all seasons. In cases where the major consumptions are during the night and morning, the system has to be slightly oversized with a larger PV/T area and larger heat pump capacity and storing about one-third of electrical energy generated in a battery.

Nomenclature

A: Area
C_p: Specific heat capacity
C_w: Specific heat of water
D_e: External diameter of tube
E: Electrical energy
fw: Collector efficiency factor
h: Heat transfer coefficient
hf_i: Convection of storage
I: Hourly total irradiation
k: Thermal conductivity
k_T: Clearness index
l: Length
m: Mass
$\dot{m}$: Mass flow rate of water
n: Number of days in a year
N: Number of tubes
$\dot{Q}_u$: Useful heat
T: Temperature
U_l: Overall loss coefficient
V: Volume
V_{wind}: Wind velocity.

Greek Symbols

δ: Declination angle
φ: Packing factor
$\varnothing$: Latitude of the location
ρ: Density
ρ_g: Ground reflection
β: Inclination angle
ϖ: Hour angle
η_f: Fin efficiency

η_r: Reference cell efficiency
$\alpha\tau$: Effective absorptance
σ: Stefan Boltzmann constant
β_r: Temperature coefficient.

Subscripts

a : Ambient temperature
b: Beam
c : Convection, inclined surface
cd: Conduction
d: Diffuse
el, a: Annual electrical
f: Fluid
g : Glass
hws, a: Annual hot water service
i: Inlet, insulation
o: Outlet, extraterrestrial irradiation
p: Absorber plate
p−i: Between absorber and insulation
P_{el}: Electrical power
pv_t, a: Annual photovoltaic thermal
r: Irradiation, reference
st: Storage
t: Time, thickness
th, a: Annual thermal
w: Water
wt: Water tube.

Abbreviations

AA: Addis Ababa city
DD: Dire Dawa city
DWC: Daily hot water consumption
FF_{ii}: Daily hot water consumption hourly fraction
pv: Photovoltaic panel
pvt: Hybrid photovoltaic thermal
TRNSYS: Transient system simulation
PVsyst: Photovoltaic sizing software.

Data Availability

Weather data (solar radiation, temperature, and sunshine hours) was collected from the Ethiopian Metrological Agency.

Conflicts of Interest

All authors declare no conflicts of interest in this paper.

References

[1] S. Abdul-Ganiyu, D. A. Quansah, E. W. Ramde, R. Seidu, and M. S. Adaramola, "Investigation of solar photovoltaic-thermal (PVT) and solar photovoltaic (PV) performance: a case study in Ghana," *Energies*, vol. 13, no. 11, p. 2701, 2020.

[2] G. Fang, H. Hu, and X. Liu, "Experimental investigation on the photovoltaic-thermal solar heat pump air-conditioning system on water-heating mode," *Experimental Thermal and Fluid Science*, vol. 34, no. 6, pp. 736–743, 2010.

[3] D. Carbonell, M. Y. Haller, D. Philippen, and E. Frank, "Simulations of combined solar thermal and heat pump systems for domestic hot water and space heating," *Energy Procedia*, vol. 48, pp. 524–534, 2014.

[4] D. Zogg, *Fault Diagnosis for Heat Pump Systems*, Swiss Federal Institute of Technology Zurich, 2002.

[5] K. Gram-Hanssen, T. H. Christensen, and P. E. Petersen, "Air-to-air heat pumps in real-life use: are potential savings achieved or are they transformed into increased comfort?," *Energy and Buildings*, vol. 53, pp. 64–73, 2012.

[6] S. Poppi, N. Sommerfeldt, C. Bales, H. Madani, and P. Lundqvist, "Techno-economic review of solar heat pump systems for residential heating applications," *Renewable and Sustainable Energy Reviews*, vol. 81, pp. 22–32, 2018.

[7] H. Nam, C. Bai, and J. Sim, "A study on characteristics of thermal storage tank for varying thermal load in multi-use heat pump water heater," *Applied Thermal Engineering*, vol. 66, no. 1–2, pp. 640–645, 2014.

[8] A. James, M. Mohanraj, M. Srinivas, and S. Jayaraj, *Thermal analysis of heat pump systems using photovoltaic-thermal collectors: a review*, vol. 144, no. 1, 2021Springer International Publishing, 2021.

[9] S. Ito, N. Miura, and K. Wang, "Performance of a heat pump using direct expansion solar collectors1Paper presented at the ISES Solar World Congress, Taejon, South Korea, 24–29 August 1997.1," *Solar Energy*, vol. 65, no. 3, pp. 189–196, 1999.

[10] B. J. Ã. Huang and C. P. Lee, "Long-term performance of solar-assisted heat pump water heater," *Renewable Energy*, vol. 29, pp. 633–639, 2004.

[11] J. Ji, K. Liu, T. T. Chow, G. Pei, W. He, and H. He, "Performance analysis of a photovoltaic heat pump," *Applied Energy*, vol. 85, no. 8, pp. 680–693, 2008.

[12] J. Ji, G. Pei, T. T. Chow et al., "Experimental study of photovoltaic solar assisted heat pump system," *Solar Energy*, vol. 82, no. 1, pp. 43–52, 2008.

[13] S. Bae, S. Chae, and Y. Nam, "Performance Analysis of Integrated Photovoltaic-Thermal and Air Source Heat Pump System through Energy Simulation," *Energies*, vol. 15, no. 2, p. 528, 2022.

[14] P. Mi, J. Zhang, Y. Han, and X. Guo, "Study on energy efficiency and economic performance of district heating system of energy saving reconstruction with photovoltaic thermal heat pump," *Energy Conversion and Management*, vol. 247, article 114677, 2021.

[15] S. Lu, R. Liang, J. Zhang, and C. Zhou, "Performance improvement of solar photovoltaic/thermal heat pump system in winter by employing vapor injection cycle," *Applied Thermal Engineering*, vol. 155, pp. 135–146, 2019.

[16] S. Vaishak and P. V. Bhale, "Photovoltaic/thermal-solar assisted heat pump system: current status and future prospects," *Solar Energy*, vol. 189, pp. 268–284, 2019.

[17] S. Akmese, G. Omeroglu, and O. Comakli, "Photovoltaic thermal (PV/T) system assisted heat pump utilization for milk pasteurization," *Solar Energy*, vol. 218, pp. 35–47, 2021.

[18] A. Miglioli, N. Aste, C. Del Pero, and F. Leonforte, "Photovoltaic-thermal solar-assisted heat pump systems for building applications: integration and design methods," *Energy and Built Environment*, 2021.

[19] K. Wang, N. Li, J. Peng, and Y. He, "Study on the optimizing operation of exhaust air heat recovery and solar energy combined thermal compensation system for ground-coupled heat

pump," *International Journal of Photoenergy*, vol. 2017, Article ID 6561797, 19 pages, 2017.

[20] A. T. Eneyaw and D. A. Amibe, "Annual performance of photovoltaic-thermal system under actual operating condition of Dire Dawa in Ethiopia," *AIMS Energy*, vol. 7, no. 5, pp. 539–556, 2019.

[21] J. A. Duffie, W. A. Beckman, and W. M. Worek, *Solar Engineering of Thermal Processes*, vol. 116John Wiley & Sons, Inc, 4nd edition, 2003.

[22] S. Bhattarai, J. H. Oh, S. H. Euh, G. Krishna Kafle, and D. Hyun Kim, "Simulation and model validation of sheet and tube type photovoltaic thermal solar system and conventional solar collecting system in transient states," *Solar Energy Materials and Solar Cells*, vol. 103, pp. 184–193, 2012.

[23] T. T. Chow, W. He, J. Ji, and A. L. S. Chan, "Performance evaluation of photovoltaic-thermosyphon system for subtropical climate application," *Solar Energy*, vol. 81, no. 1, pp. 123–130, 2007.

[24] M. B. Ammar and M. B. A. M. Chaabene, "A dynamic model of hybrid photovoltaic/thermal panel," *International Renewable Energy Congress*, vol. 1, pp. 19–24, 2009.

[25] A. Bekele, D. Alemu, and M. Mishra, "Large-scale solar water heating systems analysis in Ethiopia: a case study," *International Journal of Sustainable Energy*, vol. 32, pp. 1–22, 2011.

[26] M. S. Hossain, A. K. Pandey, J. Selvaraj, N. Abd Rahim, A. Rivai, and V. V. Tyagi, "Thermal performance analysis of parallel serpentine flow based photovoltaic/thermal (PV/T) system under composite climate of Malaysia," *Applied Thermal Engineering*, vol. 153, pp. 861–871, 2019.

[27] T. L. Bergman, T. L. Bergman, F. P. Incropera, D. P. Dewitt, and A. S. Lavine, *Fundamentals of Heat and Mass Transfer*, vol. 39no. 5, 2008John Wiley & Sons, Seven edition, 2008.

[28] H. Chen, S. B. Riffat, and Y. Fu, "Experimental study on a hybrid photovoltaic/heat pump system," *Applied Thermal Engineering*, vol. 31, no. 17–18, pp. 4132–4138, 2011.

[29] M. Sardarabadi, "Computer modelling and experimental validation of a photovoltaic thermal (PV/T) water based collector system," in *2nd International Conference on Power and Energy Systems (ICPES2012)*, vol. 56, pp. 75–79, 2012.

[30] A. T. Eneyaw, "Performance analysis of hybrid photovoltaic thermal and heat pump system using computational model," June 2022 Available: http://etd.aau.edu.et/handle/123456789/24396.

[31] N. M. Abd Rahman, L. C. Haw, M. H. Jamaludin et al., "Field study of hybrid photovoltaic thermal and heat pump system for public hospital in the tropics," *Case Studies in Thermal Engineering*, vol. 30, article 101722, 2022.

[32] D. Jiang, H. Cui, R. Sun, and W. Lin, "Study fuzzy variable supplied water temperature control for air-to-water heat pumps connected to a residential floor heating system," in *IOP Conference Series: Earth and Environmental Science*, vol. 467no. 1, Article ID 012192IOP Publishing.